International Journal of Mechanical, Industrial and Aerospace Sciences
ISSN: 2517-9950
Vol:5, No:10, 2011

Feasibility Study of a BLDC Motor with Integrated Drive Circuit

Jun-Hyuk Choi, Joon Sung Park, Jung-Moo Seo, and In-Soung Jung

***Abstract*—**A brushless DC motor with integrated drive circuit for air management system is presented. Using magnetic equivalent circuit model a basic design of the motor is determined, and specific configurations are inspected thanks to finite element analysis. In order to reduce an unbalanced magnetic force in an axial direction, induced forces between a stator core and a permanent magnet are calculated with respect to the relative positions of them. For the high efficiency, and high power density, BLDC motor and drive are developed. Also vibration mode and eccentricity of a rotor are considered at the rated and maximum rotational speed Through the experimental results, a validity of the simulated one is confirmed.

***Keywords*—**blower, BLDC, inverter

I. Introduction

DC motors have ever been prominent in various industrial applications because their characteristics and controls are simple. In an industrial point of view, the dc motor is still more than others at low power ratings. However, dc motor drives have bulky construction, low efficiency, low reliability and need of maintenance. Those features are unsuitable for automotive applications.[1]

In recent years, the brushless dc (BLDC) motor is attracting growing attention for industrial applications. This is due to the total elimination of the brush/commutator assembly, which reduces audible noise and RFI problems. Moreover, BLDC motor has a number of advantages such as high efficiency, high power factor, and high power density. Recently, the motor for industrial application should be made compact and increasing the efficiency causing limited volume. Based on the technological growth of electric machines and power electronics, the trend is to replace conventional dc motor with BLDC motor based on electric motor technology.

This paper deals primarily with the design aspects of the permanent magnet brushless dc motor and drive for blower system. Experimental results from a laboratory prototype are presented to validate the feasibility of the proposed BLDC motor with integrated drives.

II. Simulation

A. Basic design

From the preceding fluid simulation of impeller device, the required characteristics of the motor, such as rotational speed and torque at rating condition, according to the output of the overall blower system are determined. Of course, we do not describe the fluid dynamics in this paper since it goes beyond the main topic of the study. Apart from the rated operations, a blower module is needed to work under maximum speed often. Table I shows the required specification of the motor. Based on the specification, first of all, rough design is conducted using magnetic equivalent circuit model [6]. Table 2 presents the designed parameters of the motor. In order to have advantage in a constant high rotation speed and cool down a heat generated from operation of long duration, we selected exterior rotor type BLDC motor.

Through a finite element analysis, performance of the designed motor is checked out and specific configurations are determined. The magnetic density distribution of the motor is expressed in Fig. 1. As can be seen in the figure, some of the rotor parts are saturated, however, considering the three dimensional structure of the rotor housing, the magnetic density of the rotor would be dispersed and decreased.

Fig. 2 shows an induced electromotive force (EMF) of the proposed motor. EMF of $15.5V_{0\text{-peak}}$ is obtained at 10,000rpm, which means the required rotational speed could be generated at input voltage of 24V. Also, a torque constant calculated from the back EMF characteristic is estimated about 14mNm/A, which could be converted a generated torque of 55mNm at rated current of 4A. With the above results, we conformed the designed motor is enough to satisfy the electromagnetic needs.

TABLE I
The Required Specifications of Motor

Items		Specifications
Motor	Input voltage [V]	24
	Rated load [mNm]	45
	Rated speed [rpm]	11,000
	Maximum load (duty 100%) [mNm]	65
	Maximum speed (duty 100%) [rpm]	14,500
	Outer diameter [mm]	≤ 60
	Efficiency [%]	≥ 70

TABLE II
The Designed Parameters of Motor

Items	Design variables
Motor type	6p / 9s outer rotor BLDC
Driving type	3 Phase 2 excited
Magnet	ND-Bonded (Br = 0.6T)
Magnet thickness [mm]	2
Outer diameter of rotor [mm]	54
Laminated stator height [mm]	12
Air gap [mm]	0.5

Jun-Hyuk Choi, Joon Sung Park, Jung-Moo Seo, and In-Soung Jung are with the Korea Electronics Technology Institute, 203-101 Bucheon-TP B/D, Yakdae-dong, Wonmi-gu, Bucheon-si, Gyeonggi-do, Korea, 420-140 (e-mail: cjh@keti.re.kr)

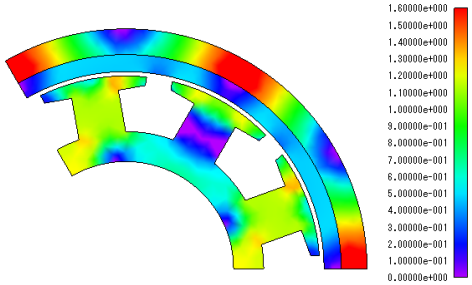

Fig. 1 Flux line and density distribution

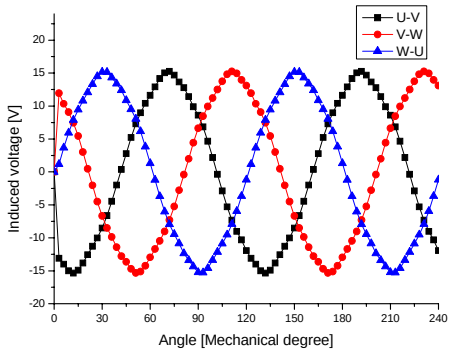

Fig. 2 Calculated back EMF waveform @ 10,000rpm

B. Electromagnetic force generated in axial direction

Due to the center distance between a stator core and a magnet as can be seen in Fig. 3, electromagnetic force could be generated in axial direction. In the case of outer rotor type motor, the force in axial direction is not zero even though the centers of them are matched each other. Because of an asymmetric cover structure, magnetic flux passed through the rotor is unbalanced in up and down side. Induced magnetic forces with respect to the relative position between permanent magnet and stator core are calculated using 3D finite element model. Fig. 4 shows the simulated results of generating force, which indicates electromagnetic force is almost zero in the axial direction in the case of the center of the stator core is about 0.5mm lower than the center of the rotor parts.

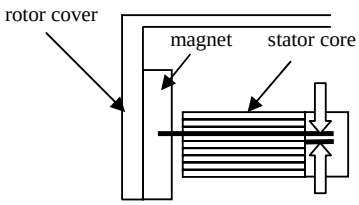

Fig. 3 Relative center distance between permanent magnet and stator core

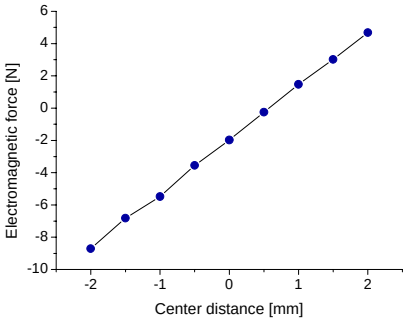

Fig. 4 Magnetic force with respect to the relative position between permanent magnet and stator core

C. Electromagnetic force generated in radial direction

When the motor has the eccentricity, flux density distribution and electromagnetic force are unbalanced, resulting in vibration and noise. Generally, the torque of rotational object is expressed as follows;

$$\mathbf{T} = \mathbf{i}_z J_z \frac{d^2\theta}{dt^2} - \mathbf{i}_x \left[j_{xz} \frac{d^2\theta}{dt^2} - j_{yz} \left(\frac{d\theta}{dt}\right)^2 \right] - \mathbf{i}_y \left[j_{yz} \frac{d^2\theta}{dt^2} + j_{xz} \left(\frac{d\theta}{dt}\right)^2 \right] \quad (1)$$

where $\mathbf{i_x}$, $\mathbf{i_y}$, $\mathbf{i_z}$ are unit vector in x, y, z axis and J_{xz}, J_{yz}, J_z are inertia of each direction. As can be seen in (1), in the case of asymmetric system there are torque components in x, y direction, and those forces are applied to a supporting part, such as bearings. The torque due to the asymmetric structure is proportional to the rotor diameter and rotation speed squared. In the proposed motor, outer diameter of the shaft is a little bigger than the conventional one having similar motor volume and rotational speed is more than 10,000rpm. Therefore, the eccentricity of the rotor could induce increasing load and bearing damage. Fig. 5 presents the electromagnetic force of the rotor in the eccentricity component direction and the orthogonal direction component against the eccentricity direction. As the eccentricity amount increases, the eccentricity direction component also increases and orthogonal direction component is unbalanced and the amplitude is larger.

D. Resonance frequency of the rotor

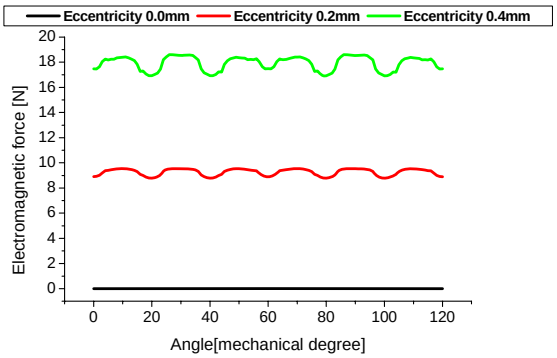

(a) Eccentricity direction component

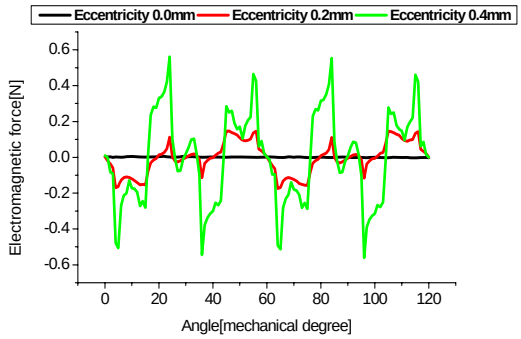

(b) Orthogonal direction component

Fig. 5 Electromagnetic force of rotor

Natural frequency of an object could affect stability of overall system. In order to investigate interference between a rotational speed and a resonance of rotor, resonance frequencies are calculated. As shown in Fig. 6, the estimated frequencies are different form the angular frequencies of the rotor which are 183.3Hz (10,000rpm) and 241.6Hz (14,500rpm).

E. Motor drive

Fig. 6 shows the typical inverter configuration and current commutation sequence. Generally, a BLDC motor is wound in a three-phase wye configuration. This configuration connects one end of each phase together to make a center point of a "Y" or the motor neutral point. This is then driven by a three-phase inverter with what is called six-step commutation. At any step, only two of the three phases are conducting current where current flows into one phase and then out another. For instance, when phase A and B conduct current, phase C is floating.

A transition from one step to another step is called commutation. So, totally, there are six steps in one cycle. As shown in Fig. 6, the first step is AB(phase A and B conducting current), then to AC, to BC, to BA, to CA, to CB and then the pattern is repeated. In order to produce maximum torque, the inverter should be commutated every 60 electrical degrees so that current is in phase with the back EMF. The conducting interval for each phase is 120 electrical degrees, or two steps. The commutation timing is determined every 60 electrical degrees by detecting when the back EMF on the floating phase crosses the zero crossing point (ZCP). The ZCP of the back EMF can be obtained by comparing the terminal voltage to the neutral point.[7]

The zero crossing technique is suitable for a wide range of applications where closed-loop operation near zero speed is not required. Its application on pumps and fans is particularly appropriate. Provided the speed is greater than zero, there are only two positions per electrical cycle when the BEMF of a phase is zero, and these positions can be distinguished by the slope of the BEMF through the zero crossing. There is a 30 electrical degree offset between the BEMF zero-crossing and required commutation positions, which must be compensated for to ensure efficient and smooth operation of the motor.

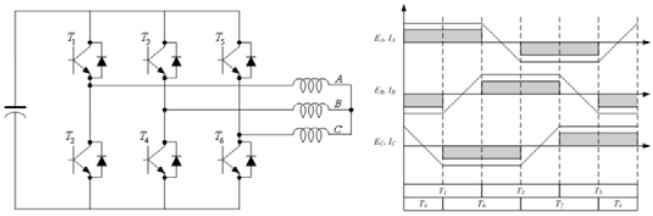

Fig. 6 Inverter configuration and current commutation sequence for BLDC

III. Experimental and Discussion

A. Characteristics measurement of proposed motor

Manufactured trial product is shown in Fig. 7. There are types of motor drives. Fig. 7 (a) shows a BLDC motor and separate drive. Fig. 7 (b) shows a BLDC motor and integrated drive. A pair of bearings is placed in up and down space of a base yoke, and a PCB for operation. Also we put a flat washer made by a Teflon material on the upper bearing, which could reduce the friction loss between the bearing and the shaft. To guarantee a stable connection an impeller with the motor, a thick shaft of the motor is required to some extent. At a high speed, the thick shaft would make wider surface area contacting the inside of bearings, it could cause a increasing friction loss. Furthermore, eccentricity should be restricted to reduce undesired forces to bearings as mentioned before. Therefore, a narrow manufacturing tolerance between the shaft and the inside of bearings is required. We manufactured the shaft and the rotor yoke separately. It means that the precise grinded shaft is put the bearings decreasing a mechanical manufacturing tolerance and rotor yoke is united with the top of the shaft. Fig. 8 shows experimental results of induced EMF at 1,000rpm and switching current of the motor. Advance switching current angle of 15 degree is set not to have a condition of current waveform distort for reduction of torque ripple and vibration.

(a) BLDC motor and separate drive

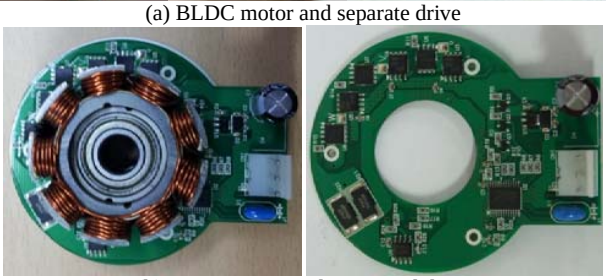

(b) BLDC motor and integrated drive

Fig. 7 Photos of the BLDC motor and drive prototype

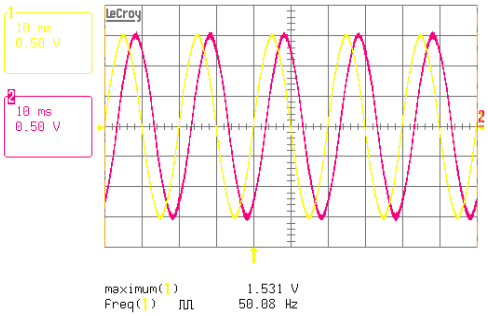

(a) Back EMF$_{\text{line to line}}$ @ 1,000rpm

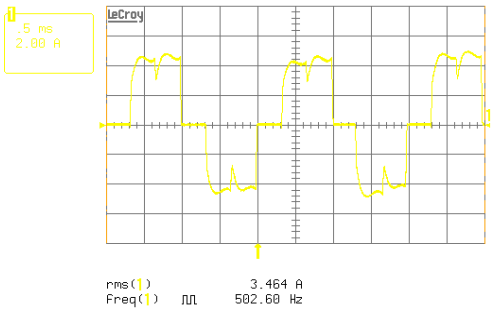

(b) Current waveform @ 10,000rpm

Fig. 8 EMF, current measurement

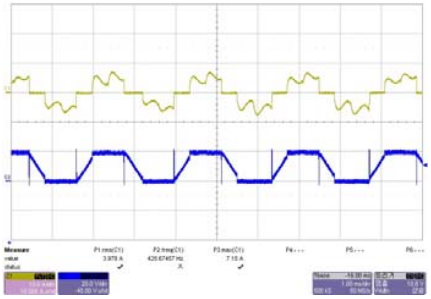

Fig. 9 Phase current and phase voltage waveform

In order to measure the characteristics of the designed motor, commercial torque detectors (EMA-1, SUGAWARA) are used and the results are shown in Fig. 10. At a rated load, rotational speed of 10,800rpm, output power of 52W, and efficiency of 73% are measured, also maximum load characteristics of 14,800rpm, 102W, 75% are obtained at input voltage of 24V. With those results, the validity of BLDC motor design for the air blower module related with an object of this study is verified.

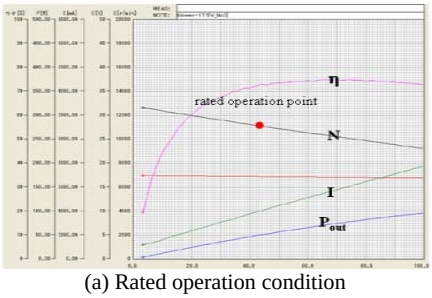

(a) Rated operation condition

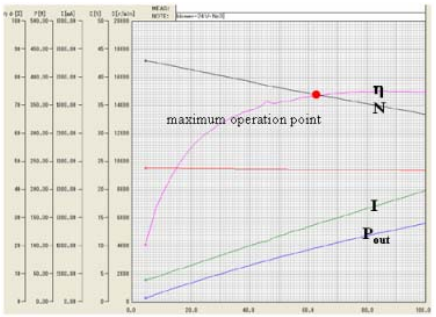

(b) Maximum operation condition

Fig. 10 Measured performance curves of BLDC motor

IV. Conclusion

This study presents a design of brushless DC motor and integrated drive for an air management system. The motor is designed by using magnetic equivalent circuit model and finite element analysis, experimental results of the manufactured motor is compared with the simulated one. Electromagnetic forces of axial and radial directions with respect to the rotor positions are calculated. Finally, output characteristics of the blower system are measured and a validity of the designed motor is confirmed.

References

[1] T.J.E. Miller, and Hendershot, Design of Brushless Permanent-Magnet Motors, Magna Physics Publishing and Clarendon Press, Oxford, 1994.
[2] Richard Valentine, Motor Control Electronics Handbook, McGrow-Hill Handbook, 1998.
[3] R. Krishnan, Electric Motor Drive, Prentice Hall, Inc, 2001.
[4] N. Kato and K. Kurozumi, "Hybrid power supply system composed of photovoltaic and fuel-cell systems," in *Proc. INTELEC'01*, Oct. 2001, pp. 631–635.
[5] M. N. Eskander and T. F. El-Shatter, "Energy flow and management of a hybrid wind/PV/fuel cell generation system," in *Proc. IEEE PESC'02*, Jun. 2002, pp. 347–353
[6] J. Hur, S. B. Yoon, D. Y. Hwang and D. S. Hyun, "Analysis of PMLSM using 3 dimensional equivalent magnetic circuit network method," *IEEE Trans on Mugnetics*, vol 33, No. 5 pp. 4143-4145
[7] J. Shao, D. Nolan, M. Tessier, and D. Swanson, "A novel microcontroller-based senserless brushless (BLDC) motor drive for automotive fuel pumps," *IEEE Trans. Ind. Appl.* Vol, 39, No. 6, pp.1734-1740, Nov./Dec. 2003.